Hindawi
Journal of Nanomaterials
Volume 2017, Article ID 4595384, 9 pages
https://doi.org/10.1155/2017/4595384

Research Article

Synthesis of ZnO Nanopowders by the Homogeneous Precipitation Method: Use of Taguchi's Method for Analyzing the Effect of Different Variables

R. Herrera-Rivera,[1] M. de la L. Olvera,[1,2] and A. Maldonado[1,2]

[1] *Programa de Doctorado en Nanociencias y Nanotecnología, Centro de Investigación y de Estudios Avanzados del Instituto Politécnico Nacional, Mexico City, Mexico*
[2] *Sección de Electrónica del Estado Sólido, Departamento de Ingeniería Eléctrica, Centro de Investigación y de Estudios Avanzados del Instituto Politécnico Nacional, Mexico City, Mexico*

Correspondence should be addressed to R. Herrera-Rivera; sharol4@hotmail.com

Received 2 August 2017; Accepted 29 October 2017; Published 29 November 2017

Academic Editor: Jean M. Greneche

In the present work the effect of different factors in the synthesis of ZnO powders by the homogeneous precipitation method is analyzed. A robust statistical technique, Taguchi's method, was used to reduce the experiments number. The variables studied were precursor, solvent and precipitating agent type, Zn molar concentration, percentage of saturation, speed and time of agitation, and temperature of synthesis. In order to optimize the particle size, an experimental design of 18 trials was proposed, according to L_{18} Taguchi array. Structural and morphological properties were characterized by X-ray diffraction (XRD) and scanning and transmission electron microscopy techniques (SEM and TEM). The estimated crystallite size in synthesized samples ranged from 32 to 57 nm. The morphologies obtained presented several forms, such as spheres, wires, flowers, bars, and tetrahedrons, with a particle size variation of 35 to 165 nm. In this work it is shown that using a statistical experimental design leads us to a fast and reliable optimization of the synthesis parameters for obtaining small size ZnO nanoparticles, thus optimizing time and human and materials resources.

1. Introduction

Zinc oxide (ZnO) is a semiconductor material that in recent years has attracted much attention due to its physical and electronic properties, such as wide direct band gap (~3.36 eV), large exciton binding energy (~60 meV), and excellent thermal stability. These properties have led to multiple applications of ZnO in various technological areas, such as optoelectronics, cosmetology, medicine, and industry [1, 2]. In addition, ZnO is a low toxicity, biocompatible and biodegradable material; these properties make possible its use in photocatalysis for water treatment [3].

On the other hand, ZnO in powder form and with nanometric dimensions presents a great potential for its application in solar cells [4], photocatalysts [5], varistors [6], and gas sensors [7], among others. There are multiple synthesis techniques for producing ZnO nanoparticles, which determine the dimensions and morphologies of the particles. Among the most reported techniques in the literature, we can mention sol-gel [8], direct and hydrothermal precipitation [9–11], aerosol process [12], sonochemical [13], microemulsions [14], mechanochemical process [15], and spray pyrolysis [9], among others. In most synthesis techniques a considerable number of variables should be considered, and the evaluation of the effect of each on the final product would require a very large number of experiments. Taguchi's method proposes a statistical experimental design that limits the number of experiments, according to the number of variables and their values (levels) to be analyzed, evaluating the effect of the variables and their magnitudes on the response of interest [1, 2, 16–20]. This statistical method is commonly applied in robust processes and allows decreasing the complexity of an experimental design, compared to other conventional techniques [19].

Table 1: List of variables and levels used in the synthesis of ZnO powders.

Variables	Levels		
	1	2	3
Zn precursor type	ZnAc	$Zn(NO_3)_2$	—
Precipitating agent type	NaOH	$(NH_4)_2CO_3$	NH_4OH
Zn molar concentration (M)	0.05	0.2	0.5
Saturation percentage (%)	5	25	50
Solvent type	DI-H_2O	CH_3-OH	CH_3-CH_2-OH
Synthesis temperature (°C)	50	70	90
Stirring speed (rpm)	300	500	1000
Stirring time (min)	30	60	120

As the new technological trends demand obtaining a high quality material with nanometric particle size, Taguchi's design is ideal in this type of processes, since we can evaluate the effect of every variable in the synthesis process with a reduced number of experiments, and from the response graphs it is also possible determine the values or levels most appropriate for each analyzed variable. Furthermore, Taguchi's method allows evaluating the effect of every variable analyzed on the measured response, as well as suggesting the optimal values, thus saving time and resources (human and materials) significantly.

In this work we propose analyzing the effect of different variables involved in the synthesis of ZnO nanoparticles by the homogeneous precipitation method, seeking to reduce the size of the particles, using Taguchi's technique. The proposal consists in analyzing the effect of eight experimental variables with three values or levels each, namely, (1) precursor type, (2) Zn molar concentration in the prepared solutions, (3) type of precipitating agent, (4) type of solvent, (5) percentage of saturation, (6) temperature of synthesis, (7) stirring rate of the solution, and (8) stirring time. The obtained nanoparticles were characterized by XRD technique, scanning electron microscopy (SEM), and transmission electron microscopy (TEM) to analyze their structural and morphological properties, respectively.

2. Experimental Details

2.1. Preparation of ZnO Nanopowders. The ZnO powders were synthesized by the homogeneous precipitation method, using two different zinc precursors at different molarities (0.05, 0.2, and 0.5 M), namely, zinc acetate, $[Zn(CH_3COO)_2 \cdot 2H_2O]$ (ZnAc), and zinc nitrate $[Zn(NO_3)_2 \cdot 6H_2O]$, and three precipitating agents with three saturation percentages each (5, 25, and 50%), sodium hydroxide [NaOH], ammonium carbonate $[(NH_4)_2CO_3]$, and ammonium hydroxide $[NH_4OH]$. The chemicals used were of reagent grade, from Sigma-Aldrich. To prepare the ZnO powders, the following procedure was carried out: (1) Zn precursors were separately dissolved in 60 ml of deionized water [DI-H_2O] under heating at different temperatures, 50, 70, and 90°C, whereas the precipitating agents were dissolved in 100 ml of deionized water [DI-H_2O], methanol [CH_3-OH], or ethanol [CH_3-CH_2-OH] at room temperature. (2) Once homogeneous solutions are obtained, the precursor solutions and precipitating solutions are mixed according to the experimental design proposed. The mixtures were stirred at different speed and time, namely, 300, 500, and 1000 rpm, during 30, 60, and 120 min. (3) Subsequently, the solutions obtained were centrifuged in an Eppendorf Model 5430, at 4500 rpm for 6 min until obtaining a solid white paste, which was thrice washed with methanol. (4) The resulting pastes were dried in air in a conventional furnace at 100°C for 1 h. (5) Finally, in order to remove the residual organic compounds, powders were calcined in air in a high temperature furnace at 400°C for 2 h. The trials were identified as S*i*, where *i* represents the trial number. The synthesis conditions used are reported in Table 1. It should be mentioned that, in trial 13, no precipitation was obtained; this result is attributed to the inhibition of the chemical reactions that lead to the ZnO formation; then in the following there are no characterization results reported for this sample.

2.2. Characterization of ZnO Powders. The structural properties of the ZnO powders were analyzed by X-ray diffraction (XRD) technique in a PANalytical diffractometer (X'PERT-PRO model), with Cu-Kα radiation (λ = 0.15406 nm). The diffraction patterns were taken in 2-theta mode (2θ) in the 30 to 80° range, with a scan step of 0.02°/min. ZnO powders were put onto on a glass slide, previously covered with carbon tape, and then protected with Parafilm, vinyl-tape. The morphological characteristics of the powders were analyzed by scanning electron microscopy (SEM microscope, HR-SEM-Auriga, Zeiss) and transmission electron microscopy (TEM microscope, JOEL, JEM-ARM200F). Particle size was statistically estimated from TEM and SEM images, using ImageJ software for SEM and Digital Micrograph for TEM.

The surface area of the ZnO powders for the samples with the most prominent morphologies (S6: bars and S7: flowers) was estimated using the BET technique (Brunauer-Emmett-Teller (BET): Micromeritics, Gemini 3240) by 12-point nitrogen adsorption. This technique provides precise specific surface area evaluation of materials by nitrogen multilayer adsorption measured as a function of relative pressure. The measurement was carried out after degassing the samples at 150°C for 2 h in N_2. The surface area data are important due to our interest in applying the synthesized

Table 2: Taguchi orthogonal matrix design, L_{18}.

ID sample	Zn precursor type	Precipitating agent type	Zn molar concentration (M)	Saturation percentage (%)	Solvent type	Synthesis temperature (°C)	Stirring speed (rpm)	Stirring time (min)
S1	1	1	1	1	1	1	1	1
S2	1	1	2	2	2	2	2	2
S3	1	1	3	3	3	3	3	3
S4	1	2	1	1	2	2	3	3
S5	1	2	2	2	3	3	1	1
S6	1	2	3	3	1	1	2	2
S7	1	3	1	2	1	3	2	3
S8	1	3	2	3	2	1	3	1
S9	1	3	3	1	3	2	1	2
S10	2	1	1	3	3	2	2	1
S11	2	1	2	1	1	3	3	2
S12	2	1	3	2	2	1	1	3
S13	2	2	1	2	3	1	3	2
S14	2	2	2	3	1	2	1	3
S15	2	2	3	1	2	3	2	1
S16	2	3	1	3	2	3	1	2
S17	2	3	2	1	3	1	2	3
S18	2	3	3	2	1	2	3	1

ZnO powders for manufacturing chemical gas sensors, since an increasing of the surface area, or presence of a porous structure, are suitable for increasing the gas sensing response.

The optical properties of the ZnO powders were analyzed using a Jasco V-670 UV-Vis spectrophotometer, in the reflectance mode, using the accessory number SLM-736. The reflectance spectra were obtained from ZnO powders contained in a quartz cuvette, in a wavelength range of 200–1100 nm. The data obtained were transformed through the Kubelka-Munk function $K = (1 - R(h\nu))^2/2R(h\nu)$ [21].

2.3. Taguchi Design. Based on the large number of variables studied and values or levels number proposed, in this work, the statistical experimental design proposed by G. Taguchi [19] was used. The Taguchi method allowed us to find out the optimal conditions for synthesizing ZnO powders. The Taguchi orthogonal matrix, L_{18} ($2^1 \times 3^7$), was used for designing the experimental trials, considering the mentioned eight variables and three different levels, with exception of precursor type (see Table 1).

It should be considered that an experimental array with eight variables and the two or three levels fixed would lead to 56 different trials or experimental combinations; however, by using a L_{18} ($2^1 \times 3^7$) Taguchi experimental design, the experimental array is reduced to eighteen trials. Consequently, it is evident that the experimental design proposed leads us to a significant time and resources reduction, since every experimental trial requires a working time around 6 h, in addition to time required for characterization of the powders.

Table 2 shows the different trials suggested by the Taguchi orthogonal matrix design, L_{18} ($2^1 \times 3^7$), that consists of nine columns reporting the ID samples and the eight variables, and 18 rows, corresponding to the trials suggested.

3. Results and Discussions

3.1. Structural Properties. The structural phase and the crystallite size were analyzed by the X-ray diffraction technique. Figure 1 shows the diffraction patterns of all synthesized ZnO samples. All diffraction peaks presented in the spectra fit well to the wurtzite hexagonal phase of ZnO, according to the crystallographic card JCPDS 36-1451 [20]. The diffraction peaks associated with the different crystallographic planes of the wurtzite phase are presented at the following angles, 2θ, 31.69 (1 0 0), 34.33 (0 0 2), 36.21 (1 0 1), 47.53 (1 0 2), 56.50 (1 1 0), 62.80 (1 0 3), 62.84 (200), 67.92 (1 1 2), and 69.03° (2 0 1). The obtained diffractograms revealed that all samples present a preferential growth in the plane (101). It should be mentioned that we cannot obtain any conclusions about the intensity magnitudes recorded, since the powder quantity analyzed was not controlled.

The crystallite size was estimated by Scherrer's equation, $D_{hkl} = c\lambda/\beta\cos\theta$, where c is a constant (~0.89), λ is the wavelength of the radiation used ($\lambda_{Cu} = 0.154$ nm), θ is

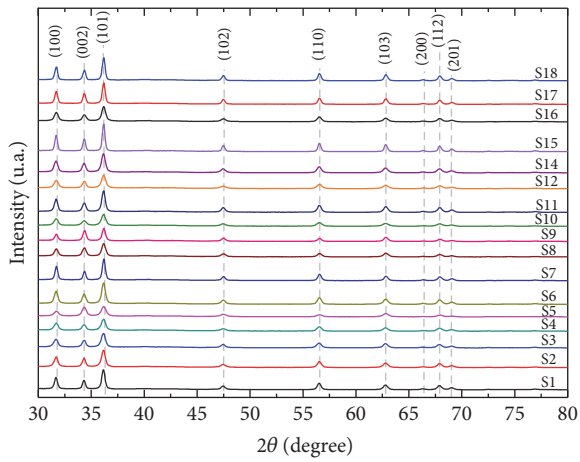

Figure 1: X-ray diffraction patterns of ZnO powders obtained at different conditions by the homogeneous precipitation method.

the diffraction angle in degrees, and β is the full width at half maximum of the diffraction peak maximum in radians (FWHM) [22]. The crystallite size in the ZnO particles presented values ranging from 32 to 57 nm. This result makes evident the influence of the magnitudes of the variables used for each experiment performed.

3.2. Morphological Properties. The morphological properties of ZnO powders synthesized by the homogeneous precipitation technique were analyzed using the scanning and transmission electron microscopy technique. SEM images with a magnification of 30.00 kX are shown in Figure 2. From the images it can be observed that ZnO powders present different morphologies, such as, spheres, wires, flowers, rods, and tetrahedral features. Particle size was estimated by using the ImageJ software. The average diameter in samples with round particles ranged from 35 to 165 nm, whereas the flower-shaped particles were 675 × 382 nm. With respect to size of wires and rods it is not possible to define their dimensions, since the SEM images do not allow seeing the particles limit.

SEM images reveal the formation of nanostructures as well as a porous surface. The most noticeable morphologies are presented in samples S5 (nanowires), S6 (nanorods), and S7 (nanoflowers). In samples S8, S9, S15, S17, and S18, particle agglomerates with a plate appearance are revealed. Samples S3 and S14 present a very porous structure, sponge-like. Additionally, samples S1, S2, S4, S10, S11, S12, and S15 show a uniform distribution with a quasi-spherical morphology. Several authors, such as Wang et al. [23], Hussain et al. [24], and Smith and Rodriguez-Clemente [25], attribute the self-assembly of ZnO in the hexagonal wurtzite phase to the dipole moment and the spontaneous polarization existing along axis c, due to the opposing charges produced by the positive charges of Zn (0001) and the negative charge of O ($000\bar{1}$). This produces a dipole-dipole interaction between the particles inducing self-assembly. The sample S5 presents the smallest particle size, around 35 nm, whereas sample S1 presents the highest value, on the order of 165 nm.

Furthermore, Zhang et al. [26] analyze the growth kinetic from the point of view of the ion-mediated classical crystal growth by atom/molecular addition. It is said that the aggregation of the particles begins after the particles reach a stable size; later nucleation occurs by colliding with other smaller particles in a random manner, leading to a self-assembly, which may occur by a random or highly oriented process. On the other hand, Sepulveda-Guzman et al. [27] proposed a scheme of self-assembly of the nanoparticles, as given in Figure 3. Table 3 reports the geometries shown in every sample.

Figure 4 shows the TEM micrographs of all the samples processed in this study, from which the shape and size of the particles can be observed with a greater detail. Because not all samples allow the TEM analysis at long times, the images present different magnification. The estimated particle sizes from TEM images are reported in Table 3.

TEM micrographs confirm the SEM results about the presented morphologies. Most of the particles present round geometry (S1, S3–S6, S8, S10, S11 and S15, S16 and S18), sample S2 is formed by particles with conic geometry, and sample S7 reveals elongated particles with a flower-petals morphology. Samples S12 and S14 show oval (ellipse) form, and, finally, samples S9 and S17 present slightly faceted particles with a hexagonal morphology.

3.3. BET Analysis. The values estimated for the surface area of the particles and the pore volume in the two analyzed samples (S6 and S7) using the BET technique were 19.1 m^2g^{-1} and 0.025 m^3g^{-1} and 18.2 m^2g^{-1} and 0.022 m^3g^{-1} for samples S6 and S7, respectively. According to the application of interest of synthesized powders, chemical gas sensors, sample S6 is the most convenient, since in a porous material the gas adsorption improves. These results are reported in Table 3.

3.4. Optical Properties. Figure 5 shows a typical reflectance spectrum of a ZnO sample. The band gap of the samples was estimated by extrapolating the linear portion between the Kubelka-Munk function and the photon energy. Band gap magnitudes oscillated around of 3.3 eV in all samples.

3.5. Analysis of the Taguchi Method. The graphs of interaction in the method of Taguchi are significant, since they are used to interpret the correlation that exists between the variables to be studied and the parameter to optimize, in our case the particle size. In Figure 6, the trend of each variable is shown graphically with the values or levels used. In these the effect of each factor (Zn precursor type, Zn molar concentration, precipitating agent type, saturation percentage, solvent type, synthesis temperature, stirring speed, and stirring time) is evaluated on the parameter to be studied.

The temperature of synthesis, velocity, and agitation time are variables that show a minor variation or slope, which is indicative of the low influence they have on the measured response. Hence, these three variables could be maintained at any of the proposed levels. On the contrary, the rest of the variables show a greater slope, which shows a more significant effect on the synthesis of the compound. The saturation percentage is the factor that presented the highest

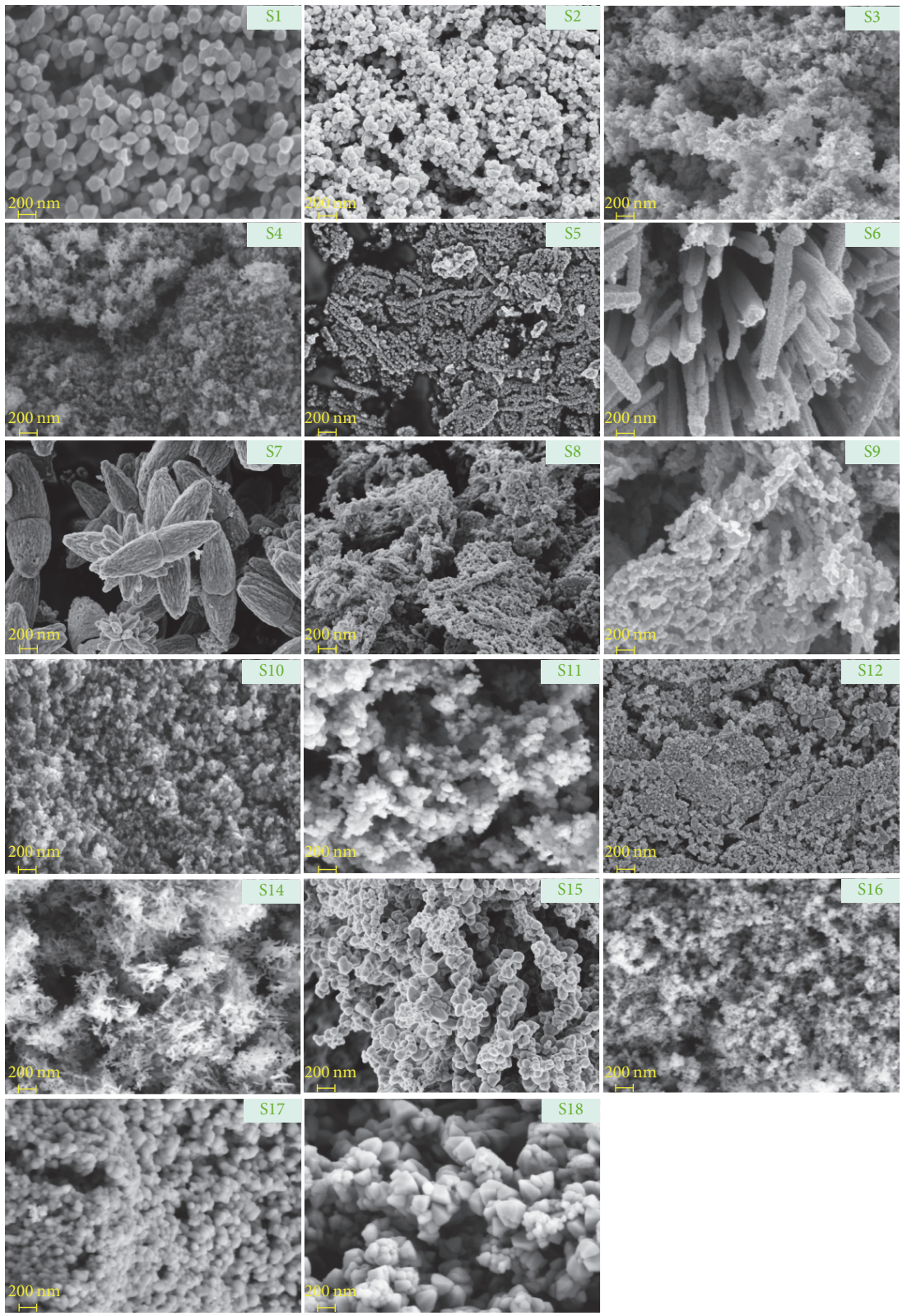

Figure 2: SEM images of ZnO powders.

Table 3: Summary of the morphological properties of ZnO powders.

ID sample	Particle shape	Particle size [nm]	BET area (m^2g^{-1})	Total pore volume (m^3/g^{-1})
S1	Spheric	164.9	—	—
S2	Spheric	66.1	—	—
S3	Spheric	45.2	—	—
S4	Spheric	37.7	—	—
S5	Wire	34.7	—	—
S6	Rod	41.6 80.0 diameter	19.1	0.025
S7	Flowers	675.0 large 370.0 base	18.3	0.022
S8	Spheric	35.1	—	—
S9	Spheric	68.7	—	—
S10	Spheric	44.9	—	—
S11	Spheric	60.2	—	—
S12	Spheric	54.0	—	—
S13	Spheric	48.2	—	—
S14	Spheric	85.4	—	—
S15	Spheric	45.4	—	—
S16	Spheric	79.1	—	—
S17	Tetrahedral	111.7	—	—

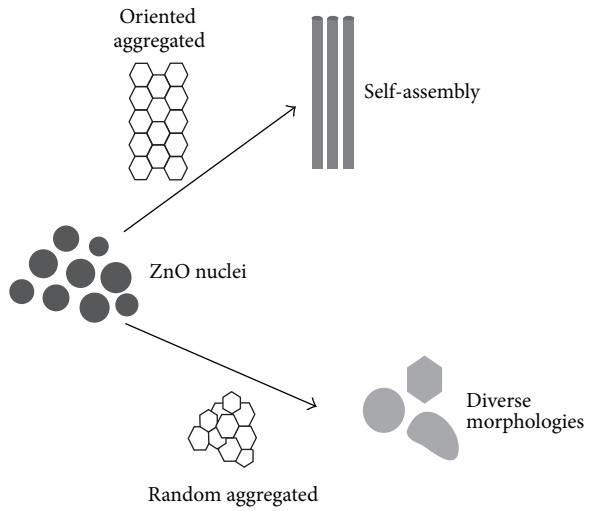

Figure 3: Schematic representation of the formation mechanism of ZnO nanoparticles processed from the homogeneous precipitation method.

influence on the particle size, on the order of 39 nm, followed by precipitating agent type, and Zn molar concentration.

4. Conclusions

The use of the Taguchi statistical technique allowed exploring the synthesis conditions that most influence the size of the ZnO nanoparticles, obtained by the homogeneous precipitation technique. The reduction in the number of experiments, from 56 to 18, led to significant time and resource savings. The particle size and shape were obtained directly from the SEM and TEM micrographs. The hexagonal wurtzite structure of ZnO powders was confirmed by X-ray diffractometry. The morphological analysis performed suggests the most suitable ZnO nanoparticles for its application in gas sensors, since there is a direct relation between surface area and gas sensitivity. From the obtained results it is evident that the homogeneous precipitation method is a potential synthesis technique for manufacturing ZnO nanoparticles with adequate particle size control. However, it is clear that more studies are needed to expand knowledge about the mechanisms of formation of nanoparticles.

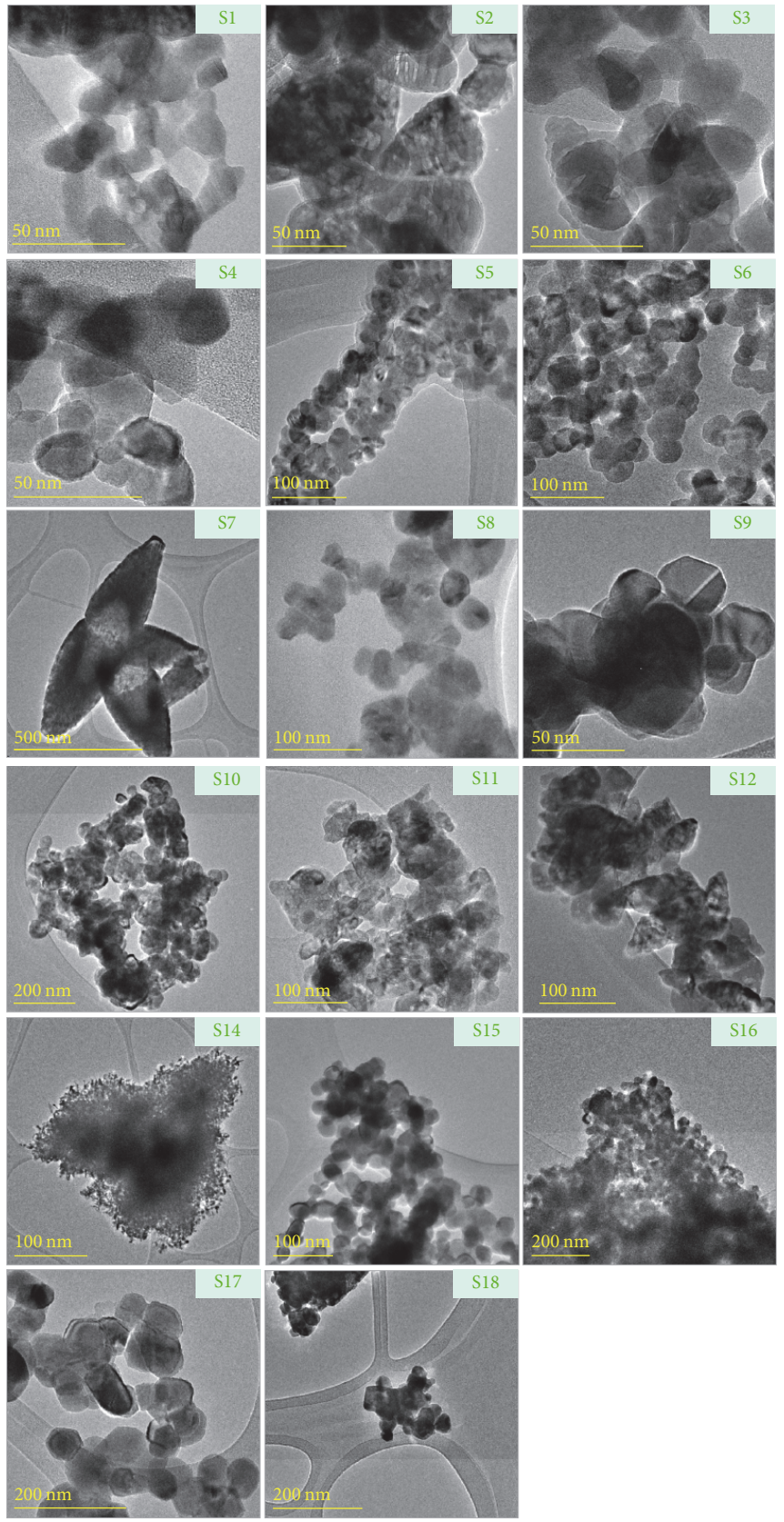

Figure 4: TEM micrographs of ZnO nanopowders.

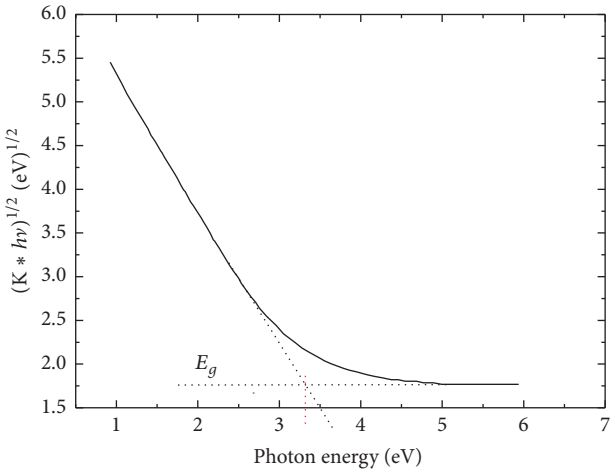

Figure 5: Plot of Kubelka-Munk function versus photonic energy of ZnO sample S16.

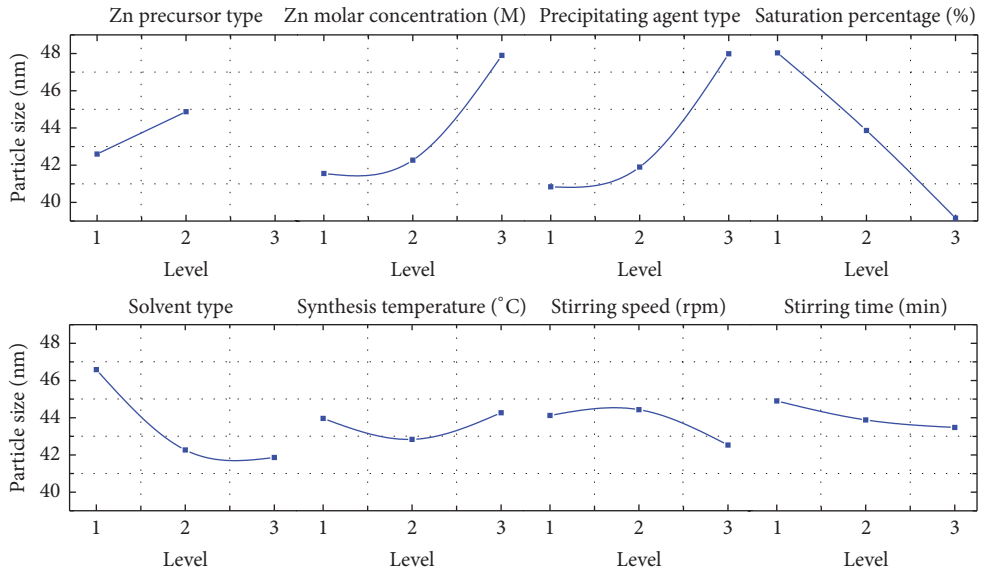

Figure 6: Interaction graphs of every variable analyzed according to the experimental design used. Effect of level value on the particle size.

Conflicts of Interest

The authors declare that they have no conflicts of interest.

Acknowledgments

The authors appreciate the support received from D. Bahena (TEM analysis) and A. Ángeles (SEM analysis) from the Advanced Laboratory of Electron Nanoscopy from CINVESTAV and A. Tavira-Fuentes (X-ray characterization). R. Herrera-Rivera also acknowledges the financial support received from CONACyT through the Ph.D. scholarship. This work was partially supported by CONACyT, through Project no. 155996.

References

[1] T. Prasad, S. Halder, M. S. Goyat, and S. S. Dhar, "Morphological dissimilarities of ZnO nanoparticles and its effect on thermophysical behavior of epoxy composites," *Polymer Composites*, 2016.

[2] N. J. Dayan, S. R. Sainkar, R. N. Karekar, and R. C. Aiyer, "Formulation and characterization of ZnO:Sb thick-film gas sensors," *Thin Solid Films*, vol. 325, no. 1-2, pp. 254–258, 1998.

[3] D. Dutta, "Optimization of process parameters and its effect on particle size and morphology of ZnO nanoparticle synthesized by sol–gel method," *Journal of Sol-Gel Science and Technology*, vol. 77, no. 1, pp. 48–56, 2016.

[4] Y. T. Chung, M. M. Ba-Abbad, A. W. Mohammad, N. H. H. Hairom, and A. Benamor, "Synthesis of minimal-size ZnO

nanoparticles through sol-gel method: Taguchi design optimisation," *Materials and Corrosion*, vol. 87, pp. 780–787, 2015.

[5] K. K. Wong, A. Ng, X. Y. Chen et al., "Effect of ZnO nanoparticle properties on dye-sensitized solar cell performance," *ACS Applied Materials & Interfaces*, vol. 4, no. 3, pp. 1254–1261, 2012.

[6] S. Akir, A. Barras, Y. Coffinier, M. Bououdina, R. Boukherroub, and A. D. Omrani, "Eco-friendly synthesis of ZnO nanoparticles with different morphologies and their visible light photocatalytic performance for the degradation of Rhodamine B," *Ceramics International*, vol. 42, no. 8, pp. 10259–10265, 2016.

[7] A. I. Ivon, A. B. Glot, R. I. Lavrov, and T. A. Bubel, "Temperature dependence of zinc oxide grain resistivity in ZnO varistor ceramics," *Journal of Alloys and Compounds*, vol. 656, pp. 740–744, 2016.

[8] P. Suchorska-Woźniak, W. Nawrot, O. Rac, M. Fiedot, and H. Teterycz, "Improving the sensitivity of the ZnO gas sensor to dimethyl sulfide," in *Proceedings of the 39th International Microelectronics and Packaging, IMAPS Poland 2015*, Poland, September 2015.

[9] G. L. Messing, S.-C. Zhang, and G. V. Jayanthi, "Ceramic powder synthesis by spray pyrolysis," *Journal of the American Ceramic Society*, vol. 76, no. 11, pp. 2707–2726, 1993.

[10] J. Wang, L. Ge, Z. Li, L. Li, Q. Guo, and J. Li, "Facile size-controlled synthesis of well-dispersed spherical amorphous alumina nanoparticles via homogeneous precipitation," *Ceramics International*, 2015.

[11] S. Baruah and J. Dutta, "Hydrothermal growth of ZnO nanostructures," *Science and Technology of Advanced Materials*, vol. 10, no. 1, Article ID 013001, 2009.

[12] T. T. Kodas, "Generation of complex Metal Oxides by Aerosol Processes: Superconducting ceramic particles and films," *Advanced Materials*, vol. 1, no. 6, pp. 180–192, 1989.

[13] A. Phuruangrat, O. Yayapao, S. Thongtem, and T. Thongtem, "Photocatalytic activity of ZNO with different morphologies synthesized by a sonochemical method," *Russian Journal of Physical Chemistry A*, vol. 90, no. 5, pp. 949–954, 2016.

[14] Ö. A. Yildirim and C. Durucan, "Synthesis of zinc oxide nanoparticles elaborated by microemulsion method," *Journal of Alloys and Compounds*, vol. 506, no. 2, pp. 944–949, 2010.

[15] L. Shen, N. Bao, K. Yanagisawa, K. Domen, A. Gupta, and C. A. Grimes, "Direct synthesis of ZnO nanoparticles by a solution-free mechanochemical reaction," *Nanotechnology*, vol. 17, no. 20, article no. 013, pp. 5117–5123, 2006.

[16] C. Jang, Z. Ye, and Q. Jiang, "Taguchi method-optimized sputter deposition of hydrogenated gallium-doped zinc oxide films in argon/hydrogen ambient," *Materials Science in Semiconductor Processing*, vol. 30, pp. 152–156, 2015.

[17] Prasad T. and Halder S., "Optimization of parameters and its effect on size of ZnO nanoparticles synthesized by sol-gel method," *Proceedings of Fourth International Conference on Soft Computing for Problem Solving. Advances in Intelligent Systems and Computing*, vol. 336, 2015.

[18] S. M. Pourmortazavi, Z. Marashianpour, M. S. Karimi, and M. Mohammad-Zadeh, "Electrochemical synthesis and characterization of zinc carbonate and zinc oxide nanoparticles," *Journal of Molecular Structure*, vol. 1099, pp. 232–238, 2015.

[19] W. Yuin and W. Alan, Diseño robusto utilizando los métodos Taguchi. Ediciones Díaz Santos, S. A., 1997.

[20] Z. Wen, L. Zhu, Z. Zhang, and Z. Ye, "Fabrication of gas sensor based on mesoporous rhombus-shaped ZnO rod arrays," *Sensors and Actuators B: Chemical*, vol. 208, pp. 112–121, 2015.

[21] J. H. Nobbs, "Kubelka—Munk Theory and the Prediction of Reflectance," *Review of Progress in Coloration and Related Topics*, vol. 15, no. 1, pp. 66–75, 1985.

[22] U. Holzwarth and N. Gibson, "The Scherrer equation versus the 'Debye-Scherrer equation'," *Nature Nanotechnology*, vol. 6, no. 9, p. 534, 2011.

[23] J. Wang, Y. Qi, Z. Zhi, J. Guo, M. Li, and Y. Zhang, "A self-assembly mechanism for sol-gel derived ZnO thin films," *Smart Materials and Structures*, vol. 16, no. 6, pp. 2673–2679, 2007.

[24] S. Hussain, T. Liu, M. Kashif et al., "Effects of reaction time on the morphological, structural, and gas sensing properties of ZnO nanostructures," *Materials Science in Semiconductor Processing*, vol. 18, no. 1, pp. 52–58, 2014.

[25] A. Smith and R. Rodriguez-Clemente, "Morphological differences in ZnO films deposited by the pyrosol technique: effect of HCl," *Thin Solid Films*, vol. 345, no. 2, pp. 192–196, 1999.

[26] Q. Zhang, S.-J. Liu, and S.-H. Yu, "Recent advances in oriented attachment growth and synthesis of functional materials: concept, evidence, mechanism, and future," *Journal of Materials Chemistry*, vol. 19, no. 2, pp. 191–207, 2009.

[27] S. Sepulveda-Guzman, B. Reeja-Jayan, E. de la Rosa, A. Torres-Castro, V. Gonzalez-Gonzalez, and M. Jose-Yacaman, "Synthesis of assembled ZnO structures by precipitation method in aqueous media," *Materials Chemistry and Physics*, vol. 115, no. 1, pp. 172–178, 2009.